JJEES

JJEES (2026) 17 (1): 73-82
ISSN 1995-6681

Jordan Journal of Earth and Environmental Sciences

Contribution of GIS and Remote Sensing in Multicriteria Seismic Risk Assessment of Existing bridges in the Oran region of Algeria

Fatima-Zohra Baba-Hamed[1*], Farid Rahal[2], Farida Guenanou[3]

[1] Lecturer, Laboratory LM2SC. University of Sciences and Technology of Oran, Mohamed Boudiaf, Oran 31000, Algeria.
[2] Lecturer, Laboratory of Analysis and Application of Radiations, University of Sciences and Technology of Oran, Mohamed Boudiaf, Oran 31000, Algeria.
[3] Associate teacher, Laboratory LMST. University of Sciences and Technology of Oran, Mohamed Boudiaf, Oran 31000, Algeria.

Received on 30 December 2024; Accepted on 25 August 2025

Abstract

BRIDGES are an important aspect of transportation infrastructure and are crucial for keeping networks working during earthquakes. However, numerous past disasters have demonstrated that vigorous tectonic activity increases the likelihood of earthquake damage to these bridges. This paper presents a unified framework for evaluating the seismic risk of existing bridges by integrating the Analytic Hierarchy Process (AHP), Geographic Information Systems (GIS), and remote sensing techniques.

The method uses eight factors to assess both the risk of earthquakes and the weakness of structures. Four of these factors are related to seismic hazard: peak ground acceleration (PGA), closeness to active faults, topographic slope, and soil classification. The other four are related to structural vulnerability: seismic design, structural type, degradation state, and functional importance based on traffic.

The method was utilized in Algeria's Oran area. Risk maps were generated for two return periods: one for 100 years and one for 475 years. The mean scenario for the 100-year return period had a PGA of 0.068 g, and the worst-case scenario had a PGA of 0.095 g. The average case for a 475-year return period was PGA = 0.138g, and the worst case was PGA = 0.18g.

The data indicate that many bridges are at significant risk during the most severe earthquake conditions. This risk is significantly greater for older structures, those exhibiting deterioration, or those inadequately designed for seismic loads, particularly when located on soft soils, or in proximity to active faults.

The suggested integrated strategy makes it easier to decide which intervention measures to focus on first. It is also a valuable tool for strengthening transportation infrastructure against earthquakes.

Keywords: *Seismic Risk Assessment; Bridges; Geographic Information Systems (GIS); Remote Sensing (RS); Multicriteria Decision Analysis (MCDA); Analytical Hierarchy Process (AHP).*

1. Introduction

One of the most deadly natural catastrophes is an earthquake. It can harm people, the economy, and the environment significantly (Al-Dogom et al., 2021). They are especially dangerous in places with high seismic activity and weak infrastructure because they can erupt unexpectedly, are challenging to predict, and can trigger other problems.

Geographic Information Systems (GIS) provide a robust framework for the management and analysis of earthquake-related datasets (Erdik et al., 2010; Kim, 1993; Kiremidjian et al., 2007; Al-Dogom et al., 2021; Almasri et al., 2024; Singh et al., 2016; Cheddad et al., 2025), while Remote Sensing (RS) delivers accurate spatial data on topography and lithology, which are critical inputs for seismic hazard modeling. Several studies (Baillifard et al., 2003; Pitilakis, 2004; Theilen-Willige, 2010; Theilen-Willige and Burnett, 2011; Galy et al., 2013; Braganza et al., 2016; Farzam et al., 2018; Farzam et al., 2021) have demonstrated that satellite-derived products are effective for analyzing site effects, particularly in how local terrain and geological conditions can amplify ground motion.

In this context, Multi-Criteria Decision Analysis (MCDA), particularly the Analytical Hierarchy Process (AHP), provides a robust methodology for weighting various aspects (Almasri et al., 2024; Sinha et al., 2016). Its integration with GIS and RS enables the production of composite risk maps, transforming complex datasets into practical decision-making tools.

Past earthquakes have shown that transportation networks, especially bridges, are highly vulnerable to seismic disasters. The 1971 San Fernando earthquake, the 1989 Loma Prieta earthquake, and the 1994 Northridge earthquake in the United States; the 1995 Kobe earthquake in Japan; and other

* Corresponding author e-mail: fatimazohra.babahamed@univ-usto.dz

destructive events around the world, such as El Asnam 1980, Costa Rica 1990, Kocaeli 1999, Taiwan 1999, and Chile 2010 (Anderson et al., 1996; Mitchell et al., 1991; Mitchell et al., 1995; Mitchell et al., 2013; Yashinsky, 1998; Priestley et al., 1994; Priestley et al., 1996). These events caused significant damage or the collapse of multiple steel and reinforced concrete bridges, which indicates how readily they may be harmed by seismic loads.

Bridges should, in principle, be able to withstand earthquakes. A lot of the bridges that are still standing were built before modern seismic guidelines were implemented, making them exceptionally unstable.

Algeria is a very difficult place since the African and Eurasian plates intersect there, which makes the seismotectonic environment quite intricate. Over the years, the country has suffered many earthquakes that caused significant damage (CRAAG, 1994; Baba-Hamed et al., 2013). The 1716 Algiers earthquake (epicentral intensity X), the 1825 Blida earthquake (intensity IX), the 1790 Oran earthquake (intensity XI), and the 1889 Mascara earthquake (intensity IX) are some of these earthquakes. There have been more recent earthquakes that have caused significant damage to people and structures, such as El Asnam in 1980 (Ms 7.3), Tipasa in 1989 (Ms 6.0), and Boumerdès in 2003 (Ms 6.0).

Many of Algeria's still-used bridges were built before earthquake-resistant design rules were established. Their construction makes them particularly fragile, especially in Oran, which is a large city and industrial center.

In this context, this study develops a GIS-based seismic risk assessment system for 116 bridges in Oran, integrating seismic hazards with the vulnerability information set. The parameters are integrated and weighted using AHP within an MCDA framework.

The goal is to identify the bridges most at risk, prioritize retrofitting and maintenance, and present decision-makers with a data-based tool that reveals where bridges are and strengthens Algeria's transportation network.

2. Methods

2.1 Study area

Oran is considered the second-largest city in Algeria. It is located in the northwest of the country on the shores of the Mediterranean, as shown in Figure 1. The city of Oran has an area of 2,114 km². It is a veritable economic and industrial hub, rich in both history and architecture. It is home to an international airport, three major ports (Oran, Mers-El Kebir, and Arzew), and several universities and research centers with regional and national influence. All of these activities generate significant traffic on the roads (Rahal et al., 2018).

The Oran region is characterized by two distinct types of geological formations (Benabdellah, 2011). The area between the base of Djebel Murdjajo and Misserghin contains Miocene formations. These formations consist of limestones and marl-limestones. In the lower part of the series, there are layers of fine sandstone associated with beds of yellow marl and some layers of shell limestone. To the south, the facies changes, leading to an increasing prominence of marly and clayey deposits. Quaternary deposits are located in the region of Es-Sénia, Chteibo, and Daia Morsli. These deposits consist of layers of highly gypsiferous and saline tuffaceous limestones, which are cracked and feature numerous lenses of detrital clay, silt, and loess, along with lignite.

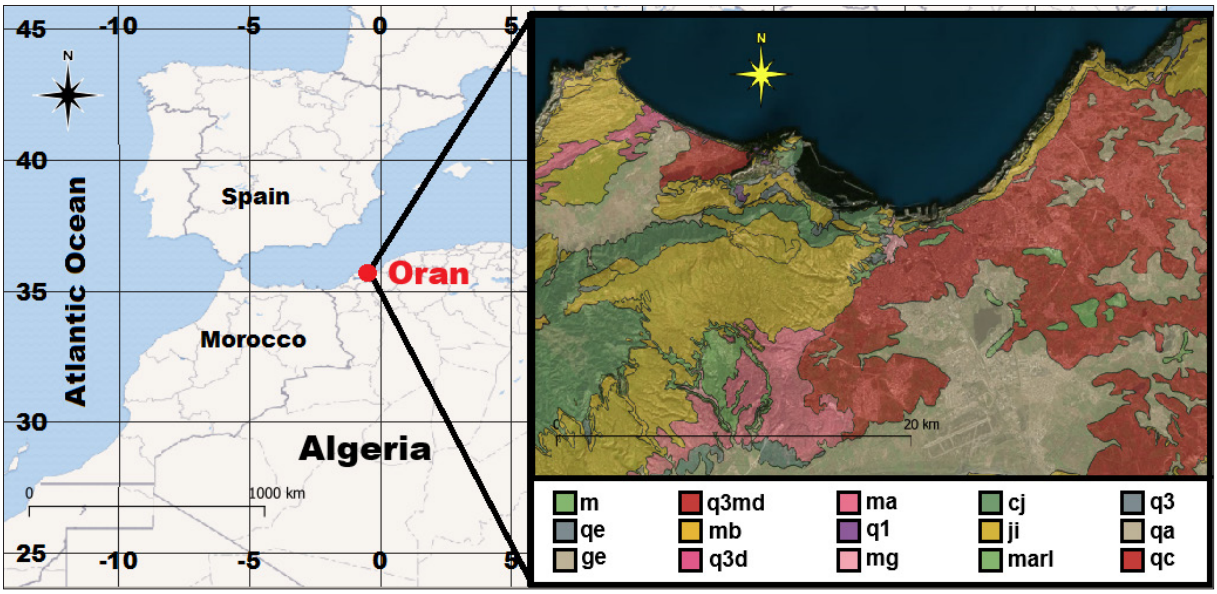

Figure 1. Geographical location of Oran city and its geological map

The altitude of Oran city increases beyond the port area as shown in Figure 2. The maximum altitude (936 m) is reached near Oued-Tlelat; the lowest, -6 m, is near the swamps of Mers-El-Hadjadj. This information appears in Figure 2, which presents the digital terrain model of Oran city.

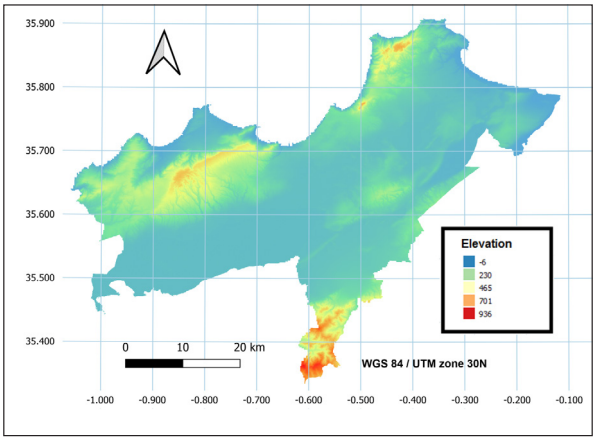

Figure 2. Elevation map of Oran city

Recent field investigations have led to the identification of two major active structures (Yelles-Chaouche et al., 2006) that can generate significant earthquakes: The Sebkha North fault spans approximately 15 km in a NE-SW direction. It delineates the Murdjadjo Mountains to the north and the vast plain of the Sebkha to the south, the Mléta basin.The Sebkha south fault extends along the Tessala Mountains for approximately 30 km in a NE–SW orientation. It intersects the piedmont surfaces represented by alluvial levels ranging from the Lower Pleistocene to the Holocene, which separate the large Sebkha of Oran (Mléta basin) to the north from the Tessala mountains to the south.

2.2 Methodology for assessing the seismic risk of bridges

This study proposes a novel framework for assessing the seismic risk of bridges in the Oran region, combining a systematic weighting method with geospatial tools, including GIS and remote sensing. The key objective is to construct a multicriteria seismic risk map that integrates both seismic hazard elements (e.g., peak ground acceleration, vicinity to active faults) and structural vulnerability characteristics (e.g., seismic design, structural condition).

In Algeria, the level of structural vulnerability is closely linked to how bridge building has changed over time, as shown in Figure 3. There are three distinct periods: before 1980, when most bridges were built with masonry, steel, or reinforced concrete without any thought to how they would hold up in an earthquake; from 1980 to 2008, when the 1980 El Asnam earthquake led to the gradual adoption of earthquake-resistant design and the implementation of the Algerian Seismic Code (RPA); and after 2008, when the introduction of a dedicated regulatory framework (RPOA) for the seismic design of engineering structures, including bridges, marked the end of the previous period.

Figure 3. Representative Bridge Structures in the Oran region

2.2.1 Decision Criteria

For a reliable seismic risk assessment, it is necessary to identify essential criteria and have access to accurate data. Eight critical criteria were selected for this study, as they were crucial for the seismic risk assessment of bridge infrastructure. These criteria are divided into two main groups: one concerns seismic hazard, the other concerns bridge vulnerability. The seismic hazard part indicates the probability and intensity of earthquakes in a given area. We selected the following factors because of their proven importance in previous studies and their availability in the studied area: Peak Ground Acceleration (PGA). We measured

PGA as the peak ground acceleration during an earthquake. It is an essential measure of seismic intensity. Regions with higher PGA values are more prone to experiencing firm ground shaking. In this study, PGA values were extracted from seismic hazard maps corresponding to return periods of 100 and 475 years, respectively, based on the maps provided by. (Peláez et al., 2003)

Distance to fault: The distance to active faults is an important factor in seismic hazard assessment, as structures located near faults are exposed to higher levels of ground shaking resulting from the sudden release of energy during fault rupture.

The fault map used in this study comes from the work of Bouhadad and Laouami (2002). Using this information, the fault proximity map is generated using QGIS software.

Slope: The steepness of a slope significantly affects the propagation and amplification of seismic waves due to topographic site effects. Slopes are classified into three groups (Borfecchia, 2016): flat surfaces, gentle slopes, or isolated reliefs with slopes less than 15° ($p < 15°$); slopes between 15° and 30° ($15° \leq p < 30°$); and steep to very steep slopes with slopes equal to or greater than 30° ($p \geq 30°$). Steeper slopes tend to accentuate ground motions in some areas, increasing the seismic threat. We used SRTM Digital Elevation Model (DEM) values to measure slope evolution over the studied area. Soil type: The lithological impacts of the site greatly influence the magnitude of ground motion amplification by local soil conditions. For example, soft soils tend to intensify seismic waves, while steep or rocky soils tend to weaken them. The Algerian Seismic Code for Works of Art (RPOA, 2008) stipulates that soil classification is generally based on parameters such as the average shear wave velocity to a depth of 30 m (Vs30) or the Standard Penetration Test (SPT) values. Table 1 summarizes these values. In this study, Vs30 values are estimated using the USGS Global Vs30 Map service, which bases its estimations on topographic slope analysis (Wald and Allen, 2007).

Table 1. Soil classification based on the Standard Penetration Test (SPT) and Average Shear Wave Velocity (Vs30)

Site Class	Soil Description	N SPT (SPT Test)	Vs(m /s) (Average Shear Wave Velocity)
S1	Rock	-	800
S2	Stiff soil	> 50	400~<800
S3	Soft soil	10~ 50	200~<400
S4	Very soft soil	<10	100~<200

Source: RPOA, 2008.

The vulnerability component denotes the intrinsic ability of a bridge to resist and dissipate seismic energy. The subsequent parameters were employed to evaluate the susceptibility of bridges:

Seismic Design: This criterion assesses if the bridge was engineered in compliance with seismic-resistant requirements.

Structural Type: This criterion pertains to the primary structural system of the bridge, encompassing the materials employed (reinforced concrete, steel, masonry) and the structural configuration (Continuous bridge, girder bridge, arch bridge, etc.). Each structure type demonstrates unique dynamic behavior and particular seismic susceptibility.

Degradation State: This parameter evaluates the current structural integrity of the bridge, based on visual inspections, technical assessments, or maintenance documentation. The degradation level is often categorized as good, fair, or poor, reflecting the extent of material deterioration or structural damage that could jeopardize the bridge's capacity to endure seismic stresses.

Functional importance: The functional importance is assessed using Average Annual Daily Traffic (AADT), an indicator of the bridge's significance in the transportation network. Bridges with elevated traffic loads are deemed operationally essential, as their failure could lead to substantial mobility disruptions and considerable socio-economic consequences.

This study utilized data from the official bridge inventory published by the Algerian Public Works Department, which offers comprehensive details on bridge location, structural type, physical condition, traffic volume, and year of construction.

2.2 .2 Analytical Hierarchy Process (AHP)

Once the criteria were identified and the spatial data collected, it became necessary to establish the relative importance of each factor in the decision-making process. For this purpose, the AHP, developed by Saaty (1980), was applied.

This method enables the transformation of expert judgments into numerical weights (Rahimi et al., 2024), taking into account both the qualitative and quantitative nature of the criteria.

The AHP approach involves three fundamental steps:

(i) The first step consists of structuring the decision problem into a multi-level hierarchical model. This study aimed to establish a hierarchy for identifying areas susceptible to seismic risk. This objective is supported by two main criteria: seismic hazard parameters and structural vulnerability parameters, each subdivided into specific sub-criteria. The hierarchisation and ranks assigned to selected factors are summarized in Table 4.

(ii) The second step involves the development of pairwise comparison matrices at each level of the hierarchy to evaluate the relative preference between factors. These comparisons were performed using a 9-point scale, where 9 indicates extreme importance, and 1 indicates an equal importance (Saaty, 1990). The matrices for the seismic hazard and vulnerability parameters are presented in Tables 2 and 3, respectively.

Table 2. Pairwise comparison matrix for seismic hazard parameters.

	Peak ground acceleration	Distance from active faults	Slope	Soil class
Peak ground acceleration	1	1	2	3
Distance from active faults	1	1	1.5	2.5
Slope percent	1/2	1/1.5	1	1.5
Soil class	1/3	1/2.5	1/1.5	1

Table 3. Pairwise comparison matrix for seismic vulnerability parameters

	Seismic Design	Structural Type	Degradation State	Functional importance
Seismic Design	1	1	1.5	3
Structural Type	1	1	1	2
Degradation State	1/1.5	1	1	2
Functional importance	1/3	0.5	0.5	1

(iii) The final step was to determine the significant eigenvalue and the related normalized eigenvector from the pairwise comparison matrices. This work was done to determine the relative weights of each parameter. To evaluate the consistency of expert judgments, the Consistency Index (CI), Random Index (RI), and Consistency Ratio (CR) were computed using the following standard formulas (Almasri et al., 2024; Sinha et al., 2016):

$$CI = \frac{\lambda_{max} - n}{n - 1} \quad \text{..... (1)}$$

$$CI = \frac{1.98(n-1)}{n} \quad \text{..... (2)}$$

$$CI = \frac{CI}{RI} \quad \text{..... (3)}$$

Where λ_{max} represents the major eigenvalue and n denotes the matrix order. A CR rating under 10% is usually considered a sign of good consistency. In this study, the calculated CR substantiates the reliability and consistency of the evaluations and the validity of the obtained weights. Table 4 shows the computed weights for the hazard and vulnerability parameters.

Table 4. Weights and ranks of the reviewed factors for hazards and vulnerability assessment

Hazard criterion			
	Class value	Rank	Weight
PGA	Inf 0.07g	1	0.36
	0.07 ≤ PGA < 0.11 g	3	
	0.11 g ≤ PGA < 0.16 g	5	
	0.16 g ≤ PGA < 0.3 g	7	
	≥0.3g	9	
Distance from active faults (Km)	<25	1	0.32
	25-50	3	
	50-75	5	
	75-100	7	
	100-125	9	
Soil class	Rock	1	0.194
	Stiff soil	3	
	Soft soil	6	
	Very soft soil	9	
Slope (degree)	<15	3	0.126
	15-30	6	
	>30	9	
CI = 0.0027	RI= 0.90	CR = 0.29%	
Vulnerability criterion			
	Class value	Rank	Weight
Seismic Design	RPOA 2008	1	0.342
	RPA	5	
	Static	9	
Structural Type	Portal frame bridge	1	0.279
	Continuous bridge	3	
	Independent Multi-Span Bridge	5	
	Composite Reinforced Concrete–Masonry Bridge	7	
	Masonry arch bridges	9	
Degradation State	Good	1	0.252
	Medium	5	
	Poor	9	
Functional importance (AADT: veh/day)	<6250	1	0.126
	6250-12500	3	
	12500-18750	5	
	18750-25000	7	
	>25000	9	
CI=0.0069	RI= 0.90	CR =0.76%	

2.2.3 Assessment of risk levels

The computed weights were incorporated into thematic raster layers within a GIS system (QGIS), with each spatial layer denoting a distinct criterion. A weighted overlay analysis was subsequently employed to create two composite indices: the Seismic Hazard Index, derived from the initial four thematic levels, and the Seismic Vulnerability Index, based on the final four layers.

The indices were computed using the corresponding derived weights. The hazard score map was classified into five levels: Negligible (0–0.2), Low (0.2–0.4), Moderate (0.4–0.6), High (0.6–0.8), and Very High (0.8–1). The hazard score map was subsequently classified into five levels: Negligible (0–0.2), Low (0.2–0.4), Moderate (0.4–0.6), High (0.6–0.8), and Very High (0.8–1). A vulnerability score map was also categorized using the same five-level scale.

The ultimate Seismic Risk Index (R) was derived as the product of the Seismic Hazard (H) and Structural Vulnerability (V) indices, as expressed in the following equation:

Risk Index = Hazard Index × Vulnerability Index .....(4)

The risk index is the hazard index multiplied by the vulnerability index. The matrix in Table 5 (CEREMA, 2016) illustrates the convergence of hazard and vulnerability levels, which establishes the seismic risk levels of bridges based on their likelihood of failure.

Table 5. Risk matrix combining hazard and vulnerability classifications

	V1	V2	V3	V4	V5
H1	R1	R1	R1	R2	R2
H2	R1	R1	R2	R3	R3
H3	R1	R2	R3	R4	R4
H4	R2	R3	R4	R5	R5
H5	R3	R4	R5	R5	R5

Where :

R1: Very- Low level risk

R2: Low-level risk

R3: Moderate-level risk

R4: High-level risk

R5: Very-High level risk

Seismic risk maps were subsequently created for several earthquake scenarios, accounting for both average and extreme Peak Ground Acceleration (PGA) values associated with return periods of 100 and 475 years.

3. Results and discussion

3.1 Evaluation of Seismic Hazard Levels

Figures 4 to 6 show the main seismic hazard parameters that are included in the GIS environment. The active fault map as shown by Figure 4, delineates bridges situated in proximity to possible rupture zones. The soil classification map (Figure 5) indicates a significant prevalence of bridges built on soft soils, hence increasing their susceptibility to seismic amplification. The slope gradient map (Figure 6) identifies slope terrains that increase ground motion.

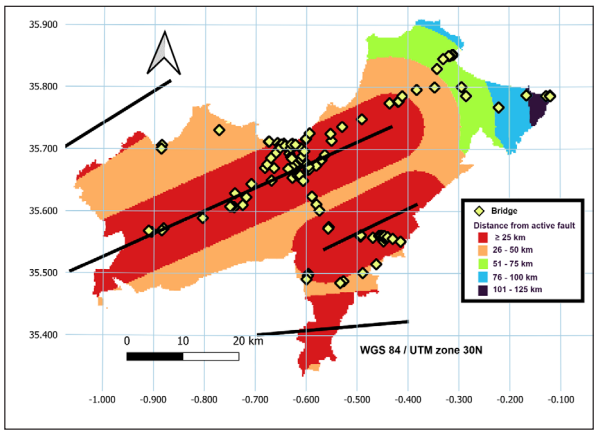

Figure 4. Distance for the active fault map in the Oran region

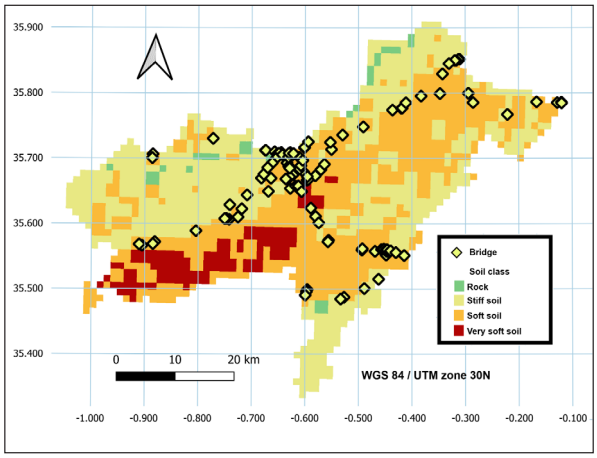

Figure 5. Soil classification map of the Oran region

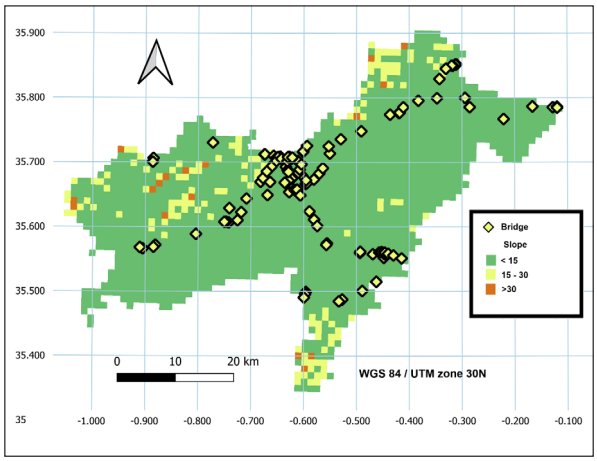

Figure 6. Slope gradient map of the Oran region

Applying the weighting strategy defined by the established method, these geographic layers were combined using a weighted overlay method within the GIS platform. The composite seismic hazard map illustrates the spatial distribution of seismic exposure, determined by active faults, terrain slope, and local soil characteristics.

Four seismic scenarios had been developed to provide a more complete evaluation of regional seismic exposure, each aligned with a specific return period and Peak Ground Acceleration (PGA) value.

• Scenario 1: Mean Peak Ground Acceleration for a 100-year Return Period (0.068 g)

• Scenario 2: Peak Ground Acceleration for a 100-year return period (0.095 g)

• Scenario 3: Average Peak Ground Acceleration for a 475-year return time (0.138 g)

• Scenario 4: Peak Ground Acceleration (PGA) for a 475-year return period (0.18 g)

Figures 7 and 8 illustrate the spatial distribution of seismic hazard levels for the analyzed bridges under four representative scenarios.

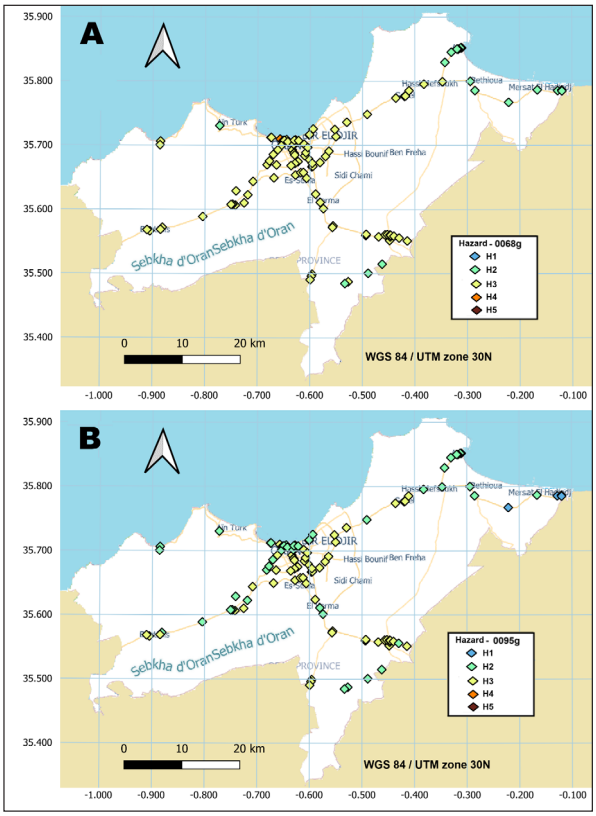

Figure 7. Mapping of seismic hazard levels of the analyzed bridges under average (PGA = 0.068g) and worst-case (PGA = 0.095g) scenarios for a 100-year return period

The comparative analysis of the four scenarios demonstrates a distinct progression in bridge exposure aligned with the increasing severity of seismic hazard.

Scenario 1 illustrates a basically secure context, with approximately 16% of bridges located in low hazard zones (H2) and 82% of bridges enduring moderate hazard levels (H3). Only 0.8% is situated in high hazard areas (H4), with no presence in the very high category (H5), signifying a limited seismic hazard.

In Scenario 2, a notable redistribution occurs: around 46% of bridges are now subjected to moderate hazard levels (H3), while an additional 50% are situated inside high hazard zones (H4). This transition indicates an increasing apprehension about structural safety.

Scenario 3 reveals an alarming situation, with over 83% of the bridge inventory in high hazard zones (H4) and the remaining 16.3% in moderate zones (H3). The lack of bridges in lower hazard categories indicates a significant rise in seismic risk.

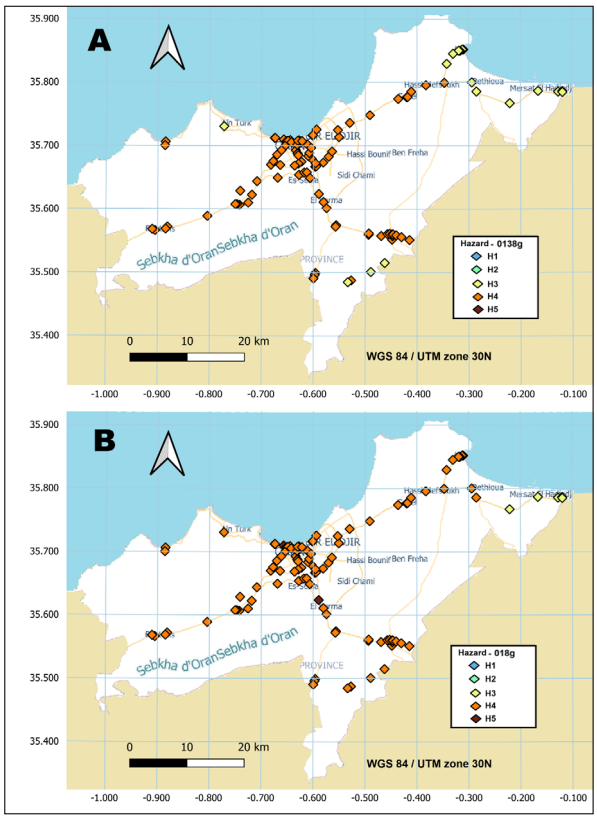

Figure 8. Mapping of seismic hazard levels of the analyzed bridges under average (PGA = 0.138 g) and worst-case (PGA = 0.18 g) scenarios for a 475-year return period

Scenario 4 represents the most critical scenario. Over 94% of bridges are located in high hazard zones (H4), while over 1.7% are in very high hazard zones (H5). Merely 4.3% persist in moderate zones (H3). This situation highlights an immediate necessity for their assessment of earthquake risk.

3.2 Seismic vulnerability Assessment of bridges

The seismic vulnerability evaluation of the bridge network was performed based on numerous critical factors outlined in the Methodology section. Figure 9 presents a visual synthesis of these criteria.

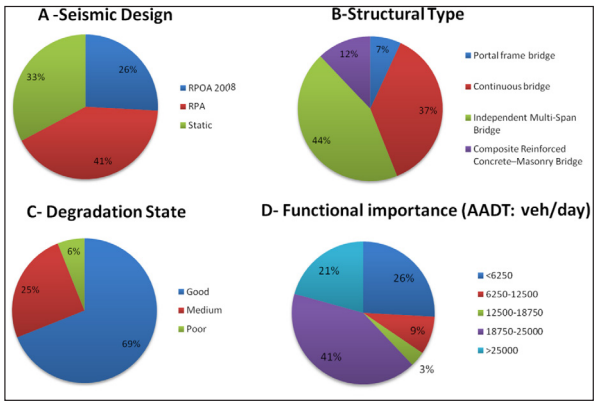

Figure 9. Graphical analysis of seismic vulnerability parameters

As illustrated in Figure 9A, significant portions, around 74%, of the bridges under study were constructed prior to the implementation of modern seismic design codes, thereby increasing their susceptibility to earthquake-induced forces.

Figure 9B indicates that the majority of the bridges studied are of conventional design, with approximately 44%

corresponding to independent multi-span bridges, which generally exhibit limited seismic performance due to their low energy dissipation capacity.

The state of degradation, shown in Figure 9C, was assessed through field inspections. The results indicate that approximately 69% of the bridges are in good condition, 25% in medium condition, and 6% in poor condition. Although the majority are in satisfactory condition, some bridges exhibit significant deterioration that negatively affects their dynamic response, meaning they require targeted maintenance and modernization.

Finally, the functional importance of each bridge, illustrated in Figure 9D, was assessed based on traffic volume and strategic role. Overall, 60% of bridges carry medium to high traffic, underscoring their key role in maintaining network connectivity.

As detailed in the Methodology section, these characteristics were weighted to reflect their relative contribution to structural vulnerability. The resultant weights were subsequently included in a GIS, facilitating a spatially referenced multicriteria analysis. This integration provided the allocation of vulnerability scores to each bridge, considering their geographic location and particular structural characteristics. Consequently, a seismic vulnerability map, illustrated in Figure 10, was produced, offering an extensive depiction of susceptibility levels over the whole bridge network.

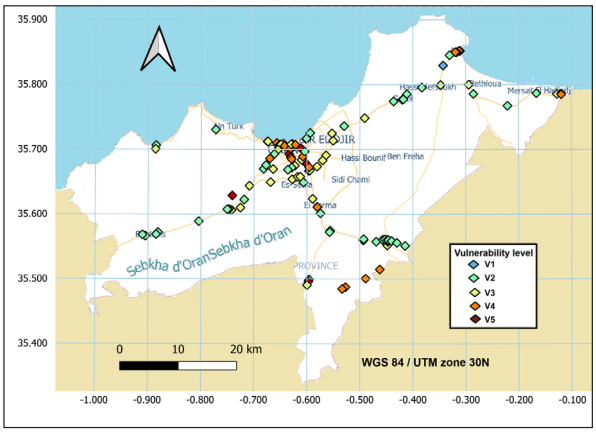

Figure 10. Map of the vulnerability levels of the inspected bridges

The analysis shows that about 38% of the bridges are in the very low to low vulnerability classifications (V1–V2), which means that their structural performance is generally satisfactory. About 33% are considered to have considerable vulnerability (V3), which means they need closer monitoringand may need to be protected. On the other hand, 29% of the bridges are in the V4–V5 range of high to very high vulnerability. They should be prioritized for intervention because their structural state is so unacceptable. The findings show that most bridges are in the moderate-to-high vulnerability classes. This result indicates the need for specific actions, such as strengthening the structure or conducting more thorough inspections, especially in areas with significant seismic hazards. Older bridges that are not reinforced for earthquakes, are built on soft soils, or exhibit structural damage are more likely to be vulnerable. In contrast, those with low vulnerabilities are generally newer constructions built in accordance with seismic design codes.

3.3 Risk Level Assessment

Seismic risk maps for each scenario were produced by integrating the hazard and vulnerability maps, as seen in Figures 11 and 12.

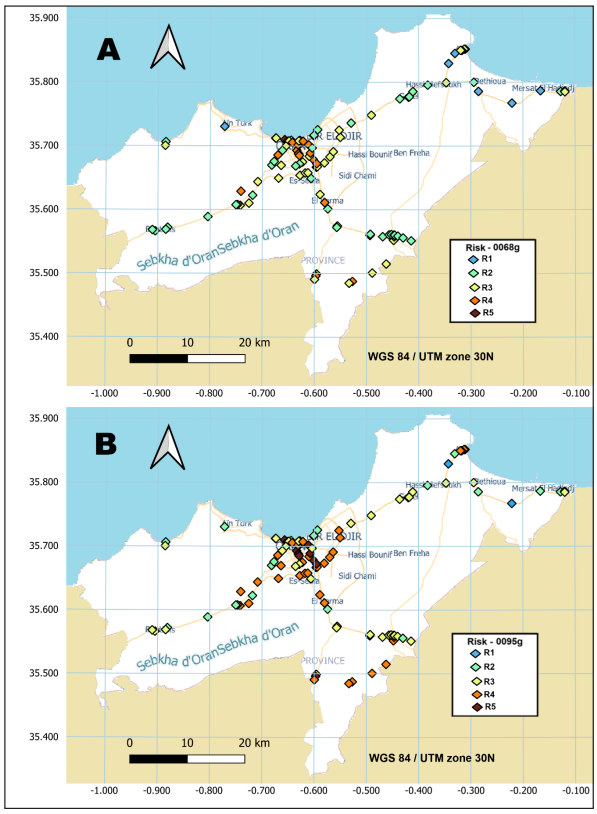

Figure 11. Mapping of seismic risk levels of the analyzed bridges under average (PGA = 0.068g) and worst-case (PGA = 0.095g) scenarios for a 100-year return period

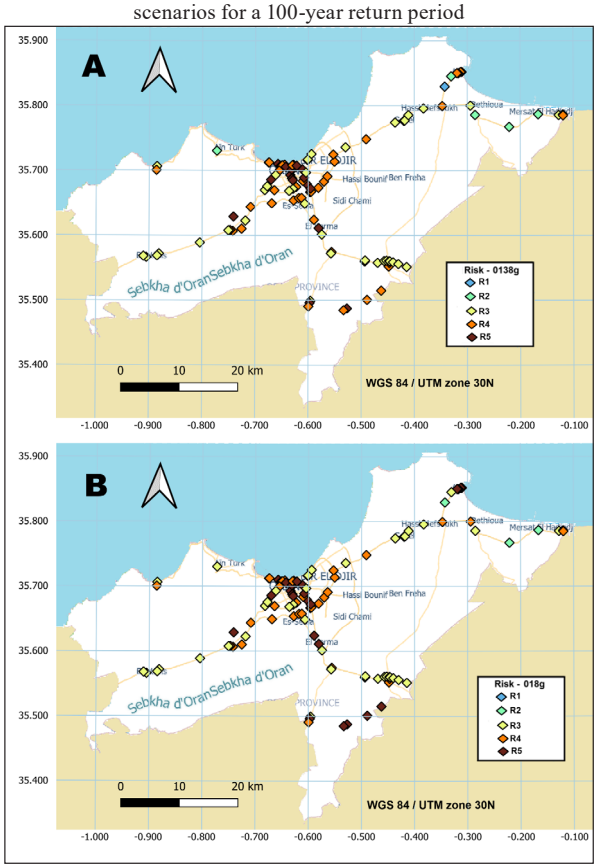

Figure 12. Mapping of seismic risk levels of the analyzed bridges under average (PGA = 0.138g) and worst-case (PGA = 0.18g) scenarios for a 475-year return period

The comparative examination of the four scenarios reveals a gradual increase in the seismic exposure of bridges as they progress from Scenario 1 to Scenario 4. In Scenario 1, most bridges are located in very low- to low-risk (40.51%) and moderate (38.80%) risk zones, with minimal presence in high (19.82%) and very high (0.86%) risk areas, reflecting a very even distribution. In Scenario 2, the distribution changes, exhibiting a substantial decline in the percentage of bridges located in lower-risk zones, with just 18.96% in very low- to low-risk and 17.24% in moderate-risk locations, while the number in high-risk (37%) and very high-risk (10.34%) zones escalates, indicating an increasing susceptibility. Scenario 3 maintains this trend, with a negligible presence in very low and low (5.17%) risk zones, a consistent proportion in moderate zones (35.34%), and a significant rise in high (38.79%) and very high (20.68%) risk categories, indicating a concerning transition into harmful areas. Finally, Scenario 4 indicates the most severe situation: no bridges exist in very low-risk places, with merely 2.58% located in low-risk zones, while 37% exist in intermediate areas. Significantly, 31% and 29.31% of the bridges are situated in high- and very-high-risk zones, respectively, highlighting the urgent necessity for immediate and extensive seismic risk assessment methods.

3.4 Discussion

The seismic risk evaluation indicates that a significant number of bridges are classified as high or very high risk. These structures are mostly located in regions with elevated seismic hazard levels and significant structural vulnerability. Such situations are commonly found near active fault lines, in areas with soft soils that amplify earthquake shaking, and near older bridges built without compliance with contemporary seismic design standards. These bridges are essential links in the infrastructure network, and their collapse following a significant earthquake could lead to severe human, economic, and logistical consequences. Extensive studies based on advanced numerical modeling (nonlinear analysis) and immediate measures, including retrofitting or replacement, are essential to improve their resilience. Bridges categorized as moderate risk necessitate meticulous monitoring. These structures are frequently exhibit moderate susceptibility and are located in areas with moderate seismic hazard. While they do not pose an immediate danger, they are vulnerable to operational degradation or service interruptions during significant earthquakes . A comprehensive evaluation grounded in state-of-the-art numerical modeling of preventive reinforcement strategies would mitigate future maintenance expenses and ensure service continuity. Bridges situated in low- and very-low risk zones are typically located in geologically stable regions and frequently have modern designs that adhere to present construction standards. However, regular evaluation and appropriate maintenance are crucial to guaranteeing their continued performance, especially given structural deterioration and altering environmental conditions. These results provide a solid basis for prioritizing intervention measures. Infrastructure managers may develop an effective and economically viable earthquake risk-reduction strategy by focusing on the most susceptible structures and by conducting continuous inspections of low-risk bridges.

4. Conclusion

The present study introduced a comprehensive technique for seismic risk assessment of bridges by integrating the AHP, GIS, and remote sensing data. The methodology used four hazard criteria (peak ground acceleration, fault proximity, topographic slope, and soil type) alongside four vulnerability criteria (seismic design, structural type, degradation state, and functional importance) to create a comprehensive, spatially explicit seismic risk map for a collection of engineering structures.

The results identified major intervention sites where bridges show structural vulnerabilities and significant hazard exposure. The established method is reproducible and adaptive, contributing as an essential decision-support tool for infrastructure managers, local authorities, and civil protection services. It simplifies resource allocation for maintenance and retrofitting while also improving emergency response strategies for potential earthquakes.

Nevertheless, specific constraints persist, especially the absence of dynamic data on bridge performance and the uncertainty surrounding the qualitative assessment of risk. The prospective combination of data from in situ sensor data with sophisticated numerical modeling (nonlinear analysis) may substantially enhance the precision of these analyses.

Conflict of Interest

The authors declare no conflict of interest.

Funding

The authors received no financial support for the research, authorship, and/or publication of this article.

References

Al-Dogom, D., Al-Ruzouq, R., Kalantar, B., Schuckman, K., Al-Mansoori, S., Mukherjee, S., & Ueda, N. (2021). Geospatial multicriteria analysis for earthquake risk assessment: Case study of Fujairah City, UAE. Journal of Sensors, 2021, Article 6638316. https://doi.org/10.1155/2021/6638316

Anderson, D. L., Mitchell, D., & Tinawi, R. G. (1996). Performance of concrete bridges during the Hyogo-ken Nanbu (Kobe) earthquake on January 17, 1995. Canadian Journal of Civil Engineering, 23, 714–726. https://doi.org/10.1139/l96-884

Baba Hamed, F. Z., Rahal, D. D., & Rahal, F. (2013). Seismic risk assessment of Algerian buildings in urban areas. Journal of Civil Engineering and Management, 19(3), 348–363. https://doi.org/10.3846/13923730.2012.744772

Baillifard, F., Jaboyedoff, M., & Sartori, M. (2003). Rockfall hazard mapping along a mountainous road in Switzerland using a GIS-based parameter rating approach. Natural Hazards and Earth System Sciences, 3, 435–442. https://doi.org/10.5194/nhess-3-435-2003

Benabdellah, M. (2011). Mise en évidence des phénomènes dynamiques contrôlant le littoral oranais (de la Calère à la Pointe de Canastel): Étape fondamentale pour une cartographie des risques géologiques (Doctoral dissertation). Université Mohamed Ben Ahmed d'Oran 2, Algeria.

Borfecchia, F., De Canio, G., De Cecco, L., Giocoli, A., Grauso, S., La Porta, L., & Zini, A. (2016). Mapping earthquake-induced landslide hazard around the main oil pipeline network of the Agri Valley (southern Italy) using GIS-based modeling approaches. Natural Hazards, 81, 759–777. https://doi.org/10.1007/s11069-015-2104-0

Bouhadad, Y., & Laouami, N. (2002). Earthquake hazard assessment in the Oran region (northwest Algeria). Natural Hazards, 26, 227–243. https://doi.org/10.1023/A:1015602815231

Braganza, S., Atkinson, G. M., Ghofrani, H., Hassani, B., Chouinard, L., Rosset, P., & Hunter, J. (2016). Modeling site amplification in eastern Canada on a regional scale. Seismological Research Letters, 87(4), 1008–1021. https://doi.org/10.1785/0220160009

CEREMA. (2016). Déclinaison régionale du cadre d'actions pour la prévention du risque sismique (CAPRiS) en région PACA (87 pp.). Centre d'Études et d'Expertise sur les Risques, l'Environnement, la Mobilité et l'Aménagement.

Cheddad, S., Haouchine, A., & Benmerabet, N. (2025). Surface runoff estimation using GIS data under HEC-HMS: Wadi Laussif sub-basin, Algeria. Jordan Journal of Earth & Environmental Sciences, 16, 220–226.

CRAAG. (1994). Les séismes en Algérie de 1365 à 1992. Centre de Recherche en Astronomie, Astrophysique et Géophysique, Algiers.

Davi, D., Kahan, M., Légeron, F., Marchand, P., Portier, B., Resplendino, J., Schmitt, P., Thibault, C., & Vivier, A. (2011). SISMOA: Évaluation préliminaire du risque sismique sur les ouvrages d'art existants (Technical report). SETRA.

Erdik, M., Sesetyan, K., Demircioglu, M., Hancilar, U., Zulfikar, C., Cakti, E., & Harmandar, E. (2010). Rapid earthquake hazard and loss assessment for the Euro-Mediterranean region. Acta Geophysica, 58, 855–892. https://doi.org/10.2478/s11600-010-0027-4

Farzam, A., Nollet, M. J., & Khaled, A. (2018). Susceptibility modeling of seismically induced effects integrated into rapid scoring procedures for bridges using GIS tools. Geomatics, Natural Hazards and Risk, 9, 589–607. https://doi.org/10.1080/19475705.2018.1466731

Farzam, A., Nollet, M. J., & Khaled, A. (2021). Integration of site condition information using GIS for seismic risk reduction of bridge networks. Georisk: Assessment and Management of Risk for Engineered Systems and Geohazards. https://doi.org/10.1080/17499518.2021.1952609

Galy, B., Khaled, A., & Nollet, M. J. (2013). Seismic vulnerability assessment of typical Quebec City bridges considering site-specific amplification. Canadian Journal of Civil Engineering, 40, 1–10. https://doi.org/10.1139/cjce-2011-0052

Kim, S. H. (1993). A GIS-based regional risk analysis approach for bridges against natural hazards (Doctoral dissertation). State University of New York at Buffalo.

Kiremidjian, A., Moore, J. E., Fan, Y., Yazlali, O., Basoz, N., & Williams, M. (2008). Seismic risk assessment of transportation network systems. Journal of Earthquake Engineering, 12(Supplement 1), 76–100.

Kibboua, A., Bechtoula, H., Mehani, Y., & Naili, M. (2014). Vulnerability assessment of reinforced concrete bridges in Algiers using scenario earthquakes. Bulletin of Earthquake Engineering, 12, 807–827. https://doi.org/10.1007/s10518-013-9523-7

Mitchell, D., Tinawi, R., & Sexsmith, R. G. (1991). Performance of bridges in the 1989 Loma Prieta earthquake—Lessons for Canadian designers. Canadian Journal of Civil Engineering, 18, 711–734. https://doi.org/10.1139/l91-085

Mitchell, D., Bruneau, M., Saatcioglu, M., Williams, M., Anderson, D., & Sexsmith, R. (1995). Performance of bridges in the 1994 Northridge earthquake. Canadian Journal of Civil Engineering, 22, 415–427. https://doi.org/10.1139/l95-050

Mitchell, D., Huffman, S., Tremblay, R., Saatcioglu, M., Palermo, D., Tinawi, R., & Lau, D. (2013). Damage to bridges due to the 27 February 2010 Chile earthquake. Canadian Journal of Civil Engineering, 40, 675–692. https://doi.org/10.1139/l2012-045

MTQ. (2013). Ouvrages d'art: Tome III—Classification des ouvrages d'art. Ministère des Transports du Québec.

OFROU. (2005). Seismic assessment of existing road bridges. Swiss Federal Roads Office.

Peláez, J. A., Hamdache, M., & Casado, C. L. (2006). Seismic hazard in terms of spectral accelerations and uniform hazard spectra in northern Algeria. Pure and Applied Geophysics, 163, 119–135. https://doi.org/10.1007/s00024-005-0011-0

Pitilakis, K. (2004). Site effects. In Recent advances in earthquake geotechnical engineering and microzonation (pp. 139–197). Springer. https://doi.org/10.1007/1-4020-2528-9_6

Priestley, M. J. N., Verma, R., & Xiao, Y. (1994). Seismic shear strength of reinforced concrete columns. Journal of Structural Engineering, 120, 2310–2329. https://doi.org/10.1061/(ASCE)0733-9445(1994)120:8(2310)

Priestley, M. J. N., Seible, F., & Calvi, G. M. (1996). Seismic design and retrofit of bridges. Wiley.

Rahal, F., Hadjou, Z., Blond, N., & Aguejdad, R. (2018). Urban growth, mobility, and air pollutant emissions in the Oran region, Algeria. Cybergeo: European Journal of Geography. https://doi.org/10.4000/cybergeo.29111

Rahimi, N., Kargaranbafghi, F., Shahid, M. R., & Afkhami, S. (2024). Using fuzzy logic and AHP for mineral potential mapping in the Janja exploration area, Iran. Jordan Journal of Earth & Environmental Sciences, 15, 275–286.

RPOA. (2008). Paraseismic rules applicable to civil engineering works. Ministry of Public Works, Algeria.

Saaty, T. L. (1980). The analytic hierarchy process. McGraw-Hill.

Saaty, T. L. (1990). How to make a decision: The analytic hierarchy process. European Journal of Operational Research, 48, 9–26. https://doi.org/10.1016/0377-2217(90)90057-I

Sinha, N., Nair, P., & Joshi, P. K. (2016). Using spatial multicriteria analysis (SMART) in earthquake risk assessment: Delhi region, India. Geomatics, Natural Hazards and Risk, 7, 680–701. https://doi.org/10.1080/19475705.2014.945100

Theilen-Willige, B. (2010). Detection of local site conditions influencing earthquake shaking using remote sensing and GIS methods in southwest Haiti. Natural Hazards and Earth System Sciences, 10, 1183–1196. https://doi.org/10.5194/nhess-10-1183-2010

Theilen-Willige, B., & Burnett, F. B. (2011). Detection of local site conditions influencing earthquake effects in the Valparaíso area, central Chile. Science of Tsunami Hazards, 30, 86–101.

Wald, D. J., & Allen, T. I. (2007). Topographic slope as a proxy for seismic site conditions. Bulletin of the Seismological Society of America, 97, 1379–1395. https://doi.org/10.1785/0120060267

Yashinsky, M. (1998). Performance of bridge seismic retrofits during the Northridge earthquake. Journal of Bridge Engineering, 3, 1–14. https://doi.org/10.1061/(ASCE)1084-0702(1998)3:1(1)

Yelles-Chaouche, A. K., Boudiaf, A., Djellit, H., & Bracene, R. (2006). Active tectonics in northern Algeria. Comptes Rendus Geoscience, 338, 126–139. https://doi.org/10.1016/j.crte.2005.11.002